American Mineralogist, Volume 87, pages 593–602, 2002

Formation of secondary pyrite and carbonate minerals in the Lower Williams Lake tailings basin, Elliot Lake, Ontario, Canada

A. DOGAN PAKTUNC* AND NAND K. DAVÉ

Canada Centre for Mineral and Energy Technology (CANMET), Mining and Mineral Sciences Laboratories, 555 Booth Street, Ottawa, K1A 0G1, Canada

ABSTRACT

The Lower Williams Lake tailings, which resulted from U-milling operations during the late 1950s and early 1960s, cover an area of 2 ha in a small bog under partial water cover. The tailings are underlain by a sand unit containing decaying organic material above the natural base consisting of sand, till, and gravel. The tailings are composed predominantly of quartz, muscovite, K-feldspar, plagioclase, and clinochlore. Residual pyrite grains, displaying angular to subangular particles measuring less than 1 to 250 μm, occur in concentrations ranging from trace to approximately 6 wt%. Framboidal pyrite has formed within the tailings basin in association with organic-rich material. The appearance of framboidal pyrite in the tailings indicates a reversal of the oxidation process and reprecipitation of Fe sulfides. In addition, the tailings include calcite, calcian siderite, Fe-oxyhydroxides, and Fe-Si-oxyhydroxides as secondary precipitates and replacement products. Groundwaters in the tailings and the underlying units are saturated with respect to gypsum and siderite. These and the other saturation indices calculated for calcite, goethite, and barite are consistent with the secondary mineralogy of the tailings. Conditions promoting the formation of pyrite can be described as neutral to weakly alkaline and reducing assisted by microbial activity. This study provides the first account of secondary carbonates and framboidal pyrite in the Elliot Lake tailings. The existing environmental conditions at the site are favorable for the desired site rehabilitation.

INTRODUCTION

The U ore mined and processed at Elliot Lake contained 3 to 8% pyrite, which ended up in the tailings. Processing of the U ore involved grinding to 50% finer than 75 μm, leaching in hot dilute sulfuric acid, and precipitation of U by anhydrous ammonia or magnesium hydroxide to form ammonium or magnesium diuranate, commonly known as yellow cake. Tailings and acidic mill waste process water were neutralized with lime and were discharged as a slurry to the tailings impoundments.

The Lower Williams Lake tailings basin, approximately 16 km north of the town of Elliot Lake, contains mill tailings from the late 1950s and early 1960s (Fig. 1). The site was reclaimed during 1976–1977 by covering the exposed tailings with a layer of glacial sand/gravel and till, and directly vegetating the surface of the applied cover. During the period between the placement of the tailings in the late 1950s and their reclamation in 1976, the tailings were oxidized to depths of 10 to 20 cm. Prior to placing the cover, the surface of the exposed tailings received a limestone amendment to neutralize the resident surface acidity. A seed mixture of agronomic species, Red Top (*Agrotis alba*) and Creeping Red Fescue (*Festuca rubra*) grasses, and inoculated Bird's Foot Trefoil (*Lotus corniculatus*) legume, was planted in the cover along with an application of an appropriate amount of high-nitrogen and phosphorus-containing fertilizer (diammonium phosphate) (Davé et al. 2000a). Today the basin supports lush vegetation of the planted agronomic as well as native species of grasses, shrubs, and trees of terrestrial, wetland, and aquatic habitats. The area is gradually turning to a natural bog representing a landform transition zone between terrestrial and aquatic habitats.

The present study was conducted as part of a project to evaluate mine-waste decommissioning options for the Denison mine waste-management areas in Elliot Lake. The purpose of the study was to determine the mineralogical composition and geochemical parameters needed in the overall assessment of the status of the geochemical evolution of the tailings site.

SITE DESCRIPTION

The tailings basin, containing approximately 20 000 tons of tailings, occupies an area of about two hectares. Approximately 70% of the area is made up of dry reclaimed tailings,

* E-mail: dpaktunc@NRCan.gc.ca

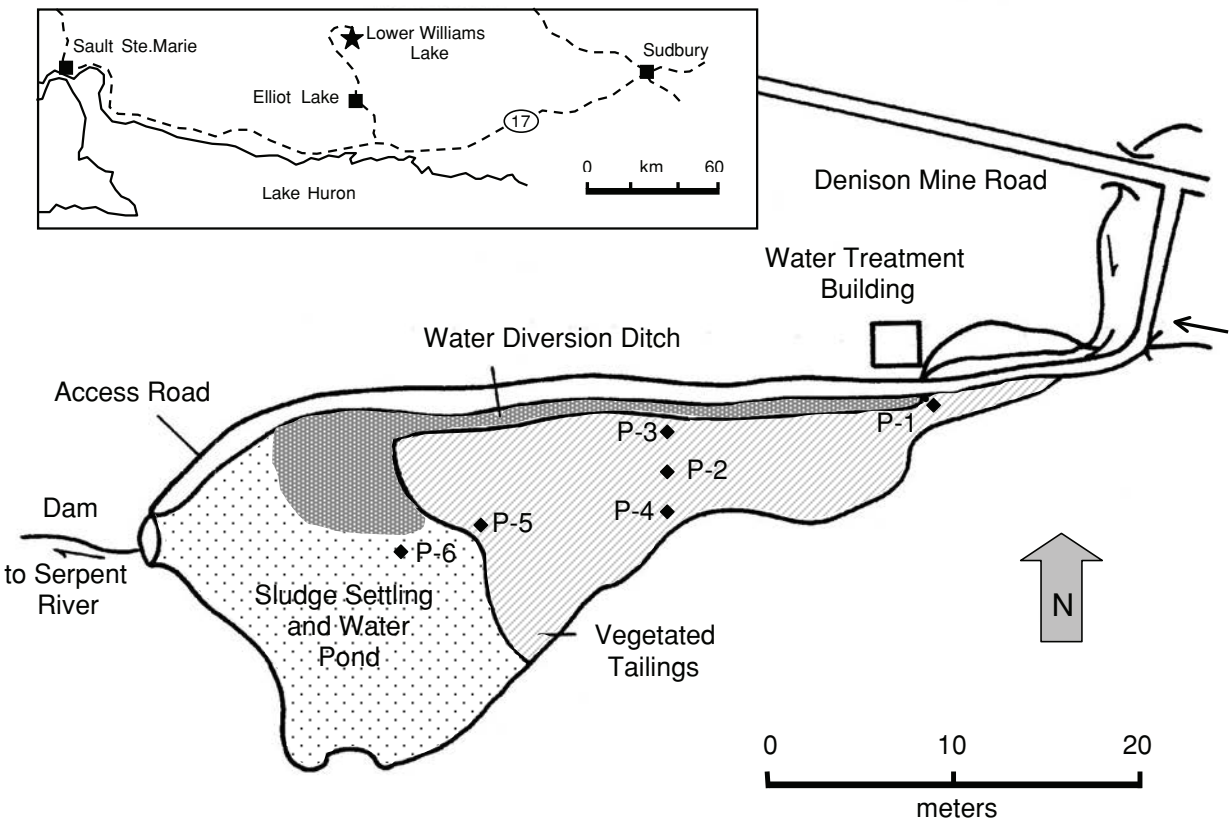

FIGURE 1. Lower Williams Lake tailings basin showing the core sampling and piezometer locations.

and the remainder of the basin consists of wetlands and ponded water areas. The thickness of the tailings in the basin ranges from approximately 0.3 to 0.85 m in the exposed area and between 0.9 and 1.25 m in the wetland and water-covered areas. The tailings are composed of fine to coarse-grained material. In general, approximately 85% of the tailings are finer than 44 µm. Accordingly, the tailings have poor draining and dewatering characteristics. The tailings are underlain by a layer of black peat and lake-bottom sediments that are approximately 0.05 to 0.3 m in thickness, followed by a layer of sand and till immediately above the bedrock (Figs. 2 and 3).

The tailings in the eastern and central parts of the basin are covered with a sand/gravel/till layer that varies in thickness from approximately 35 to 55 cm. A thin layer (less than 12 cm thick) of decaying organic plant material overlies the sand/gravel/till layer. The tailings in this area are fine- to coarse-grained and may include partly oxidized tailings having an orange coloration. The water table in this part of the basin is mostly above the tailings surface, and saturation conditions prevail through most of the tailings depth. Near the southern perimeter of the basin, however, the tailings become partly unsaturated in late summer and early fall, and this may result in some oxidation.

Tailings in the low-lying areas near the pond and water-covered portions of the basin are commonly thicker, up to approximately 1.25 m. The tailings are overlain by a thin organic layer, and the sandy cover layer is generally missing or occurs

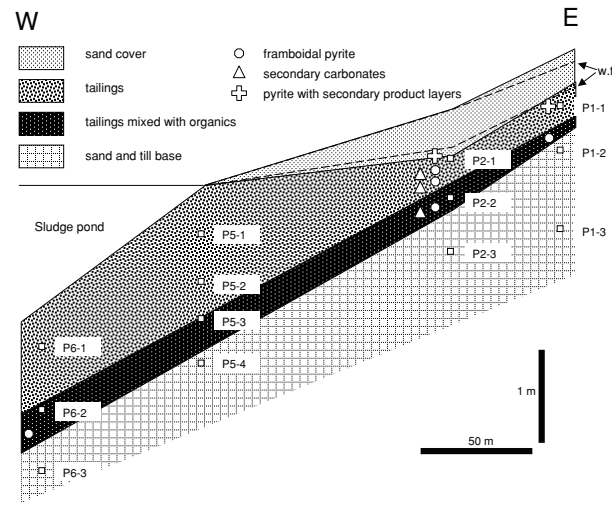

FIGURE 2. East-west cross section through the tailings basin, based on observations along the cores and piezometers. w.t = water table.

only as a thin unit. The tailings are underlain by organic-rich material. Tailings in this part of the basin consist mostly of unoxidized fine to coarse particles. Although saturated conditions prevail within the tailings, in some areas the topmost portion may become unsaturated during dry summer months. The water table rises above the surface elevation in the spring and occasionally after heavy rains, resulting in water pooling and

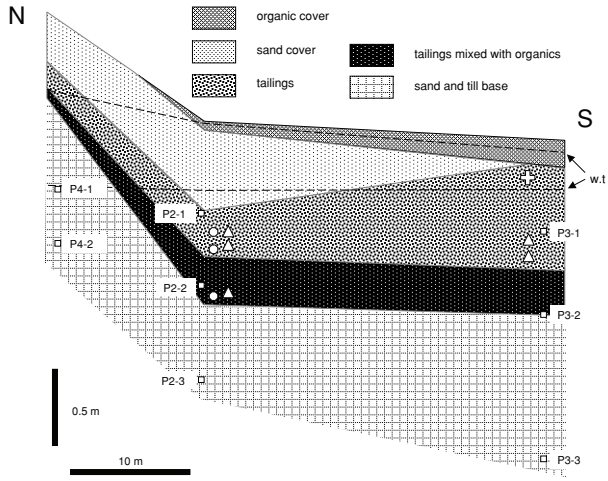

FIGURE 3. North-south cross section through the tailings basin, based on observations along the cores and piezometers. w.t. = water table.

Fe-oxyhydroxide precipitation in some parts of the site.

Submerged tailings in the eastern part of the holding pond are overlain by lime neutralization and barium chloride treatment sludge. The tailings immediately below the sludge are very fine-grained slimes. The slimes are underlain by unoxidized and compacted fine tailings. Tailings and sludge particles are generally less than 20 μm and possess angular shapes. The tailings in this location are underlain by 15 cm thick mixed layers of unoxidized tailings, sludge, bog peat, and lake sediment. The bottom of the basin is a 10 to 12 cm layer of very fine peat and lake sediment followed by a 2 to 3 cm layer of grayish clay material possibly containing some tailings.

METHODOLOGY

Six piezometer nests, each consisting of two to four individual piezometers, were installed at approximately 0.5, 1, 1.5, and 2 m depths within the tailings basin (Fig. 1). Groundwater samples were obtained on November 18, 1996, June 4, 1997, June 27, 1997, and October 6, 1997. Dissolved oxygen, pH, redox (Eh), electrical conductivity, and temperature were measured in-line using a flow-through cell during sampling. Groundwater samples were collected in bottles purged with nitrogen for laboratory measurements and chemical analysis including pH, Eh, electrical conductance, total acidity, total alkalinity, total dissolved solids, sulfate, total Fe, Fe^{2+}, Ca, Mg, Na, K, Al, Mn, U, Th, Pb, Ce, Co, Cu, Ni, Ti, V, Zn, and ^{226}Ra. While sampling, care was taken to minimize air-sample contact by slowly filling the sample bottle from the bottom to displace the head space completely. For Fe^{2+}, a small portion of the sample was separately acidified with HCl and specifically preserved in small sample bottles as above. Measurements of Fe^{2+} were made in the laboratory immediately following sampling. Details of the piezometer installation, sampling, and analytical conditions are given by Davé et al. (2000b).

A total of six core samples, each approximately 0.9 to 1.2 meters in length, were taken from locations near the piezometer installations. The sampling was conducted in February 1997, when the site was completely frozen, thereby providing easy access to wetland and water-covered locations. At each site, a continuous core sample was obtained by using a thin-walled aluminum Shelby tube, pushed into the ground to the desired depth with a percussion hammer. The extracted samples were immediately sealed at the top and bottom ends and were frozen in the field in an upright position before transporting to the laboratory. In the laboratory, each frozen core was subdivided into 30 cm sections, split into halves along the length and allowed to thaw and drain at room temperature. Individual sub-samples were oven dried at 60 °C under a nitrogen atmosphere and homogenized prior to sampling for mineralogical analysis.

The samples were studied by optical microscopy, X-ray diffraction, scanning electron microscopy, and electron microprobe analysis. The tailings samples were analyzed for their bulk Si, Ti, Al, Fe, Mg, Ca, Na, K, P, Ba, CO_2, S, and sulfate concentrations by ICP-AES, AA, and LECO techniques. Details of the analytical techniques and methodology are provided in Paktunc and Davé (1999).

Saturation indices were calculated from the pore-water chemistry data by using the PHREEQC geochemical computer program (Parkhurst 1995) and the MINTEQ database (Allison et al. 1991). Input parameters used in the calculations include temperature, pH, Eh, alkalinity, and concentrations of Si, Al, total Fe, Mg, Mn, Ca, Na, K, Ba, and sulfate concentrations. PHREEQC uses Debye-Hückel expressions to account for the non-ideality of aqueous solutions. This model is considered to be adequate for low-strength solutions (i.e., <5000 ppm total dissolved solids concentration; Langmuir 1997). Total dissolved solids concentrations in the Lower Williams Lake groundwater do not exceed 4400 ppm; therefore, the use of the Debye-Hückel model is justified. Total Fe is used in the calculations because of the analytical uncertainties in the measurement of Fe^{2+}. PHREEQ speciates total Fe using Eh measurements. The effect of the use of total Fe vs. Fe^{2+} and Fe^{3+} on the saturation indices is discussed in the following sections.

RESULTS

Mineralogy

The tailings consist of fine- to medium-grained mineral and rock particles that display angular to sub-angular shapes. The tailings are composed predominantly of quartz, muscovite, K-feldspar, plagioclase, and clinochlore. Quartz abundance is in the 50 to 60% range, and muscovite is variable from approximately 15 to 45%. K-feldspar and plagioclase occur in concentrations that are less than 4 and 16%, respectively. Monazite, rutile, ilmenite, magnetite, and a U-Ti oxide mineral, probably brannerite (UTi_2O_6), occur in minor to trace amounts.

Pyrite is the ubiquitous sulfide, occurring in variable concentrations of up to 6.3 wt%. Chalcopyrite and galena locally occur in trace quantities. There are no apparent variations of the pyrite concentration within the tailings basin other than a crude increase with depth. Pyrite occurs as angular and subangular fragments ranging in size from less than 1 to 30 μm, with a few grains up to about 250 μm. Most pyrite grains are free of other minerals but a few are enclosed in silicates. Par-

ticle margins are typically sharp and lack secondary oxidation products, but some particles have a rimmed appearance without secondary products. In general, secondary precipitates are not observed on the margins of pyrite grains; however, occasional particles of pyrite in the oxidized tailings near the surface (i.e., <0.6 m depth) display rims of secondary Fe-oxyhydroxide and hydrated Fe-sulfate. Such rims may display zoning, and some consist of multilayers of Fe-sulfate and Fe-oxyhydroxide. Iron-oxyhydroxides and hydrated Fe-sulfates also occur as irregular patches and as a matrix to quartz and muscovite particles. The presence of secondary rims, and replacement features along microfractures, is indicative of the oxidative dissolution of pyrite near the surface of the tailings affected by water-table fluctuations.

Pyrite also occurs in the form of framboids consisting of densely packed submicrometer pyrite crystals in spherical forms (Fig. 4a). Pyrite framboids range from 5 to 35 μm in diameter, and constituent pyrite crystals are 0.5 to 1.3 μm (Fig. 4b). Pyrite crystals within individual framboids are relatively uniform in size. These size ranges are similar to those reported by Wilkin and Barnes (1997) for framboids occurring in both modern sediments and sedimentary rocks. Spatial distribution of framboidal pyrite within the tailings basin is shown on Figures 2 and 3. Petrographic observations reveal that framboidal pyrite in the tailings occurs exclusively in association with organic material and the secondary minerals such as Fe-oxyhydroxides and Fe-Si-hydroxides (Fig. 4c). As shown on Figures 4a, 4b, and 4c, the framboids are free of adhering material, intact, and generally coarser than the associated tailings particles. No framboidal pyrite was found in or attached to a silicate mineral or rock particle. These textural features are strong indications for formation of framboidal pyrite in the tailings environment. Some framboidal pyrite grains are enveloped by massive pyrite (Fig. 4d). Pyrite also occurs in the form of spherical aggregates or nodules ranging in size from less than 5 to 20 μm. Larger nodules are made of framboidal pyrite surrounded by a layer of massive pyrite (Fig. 5a).

The occurrence of framboidal pyrite particles surrounded

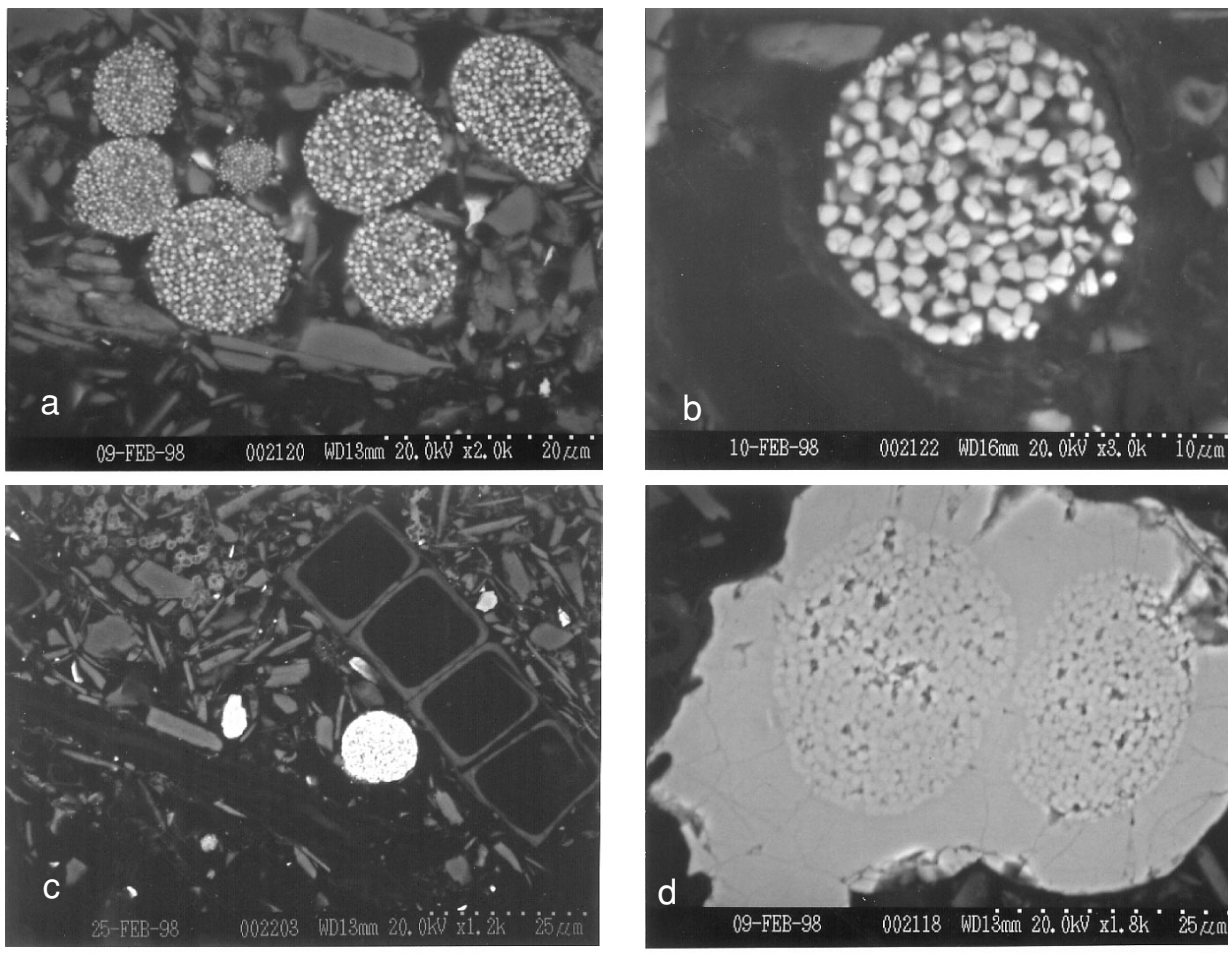

FIGURE 4. Backscattered electron photomicrographs: (**a**) Cluster of spherical and elliptical framboidal pyrite. Also present are angular pyrite grains (white), quartz, and muscovite. P2 at ~0.75 m depth; (**b**) Pyrite framboid composed of equant pyrite crystals measuring 1.3 μm. P6 at ~1.7 m depth; (**c**) Pyrite framboid, several anhedral pyrite particles (white), organic material in the form of a cellular structure, and colloid-like rings (upper left) of Fe oxyhydroxide precipitates among quartz and muscovite particles. P2 at ~1.2 m depth; (**d**) Two framboidal pyrite particles enveloped by massive pyrite. P2 at ~0.75 m depth.

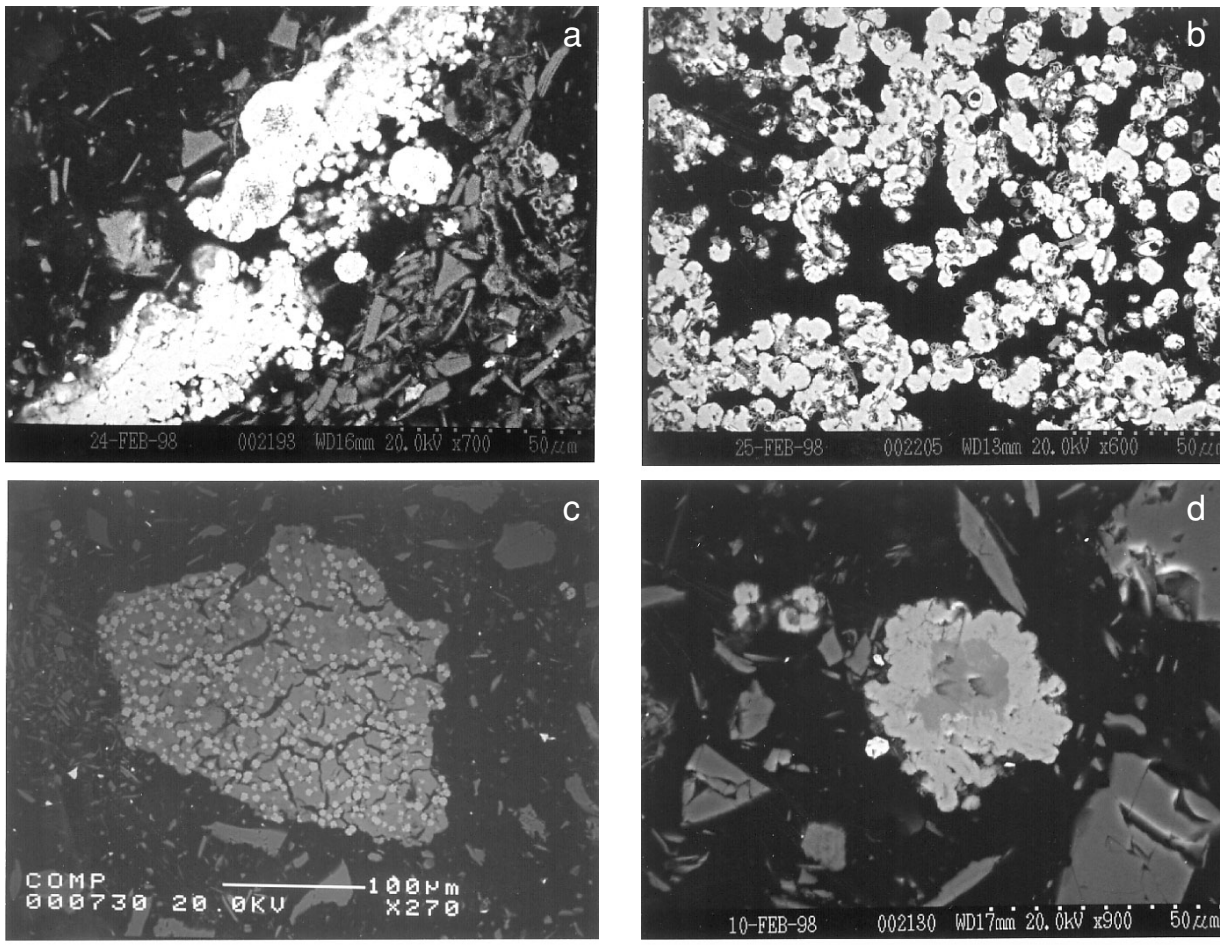

FIGURE 5. Backscattered electron photomicrographs: (**a**) Nodular pyrite grains. Note that some pyrite nodules have framboidal pyrite cores. P2 at ~0.85 m depth; (**b**) Cluster of calcian siderite nodules. P2 at ~1.2 m depth; (**c**) Calcian siderite nodules scattered in a dehydrated Fe-oxyhydroxide particle. P3 at ~0.75 m depth; (**d**) Calcian siderite nodules (light gray) as a rim on a calcite core developed around a calcite particle (dark gray). P3 at ~0.75 m depth.

by massive pyrite and of smaller pyrite particles with round outlines suggests the transformation of framboidal pyrite into massive pyrite or sequential precipitation of pyrite as single crystals. Formation of framboidal pyrite is controlled mainly by the rate that Fe monosulfides transform to pyrite (Wilkin and Barnes 1996). According to Butler and Rickard (2000), precipitation of pyrite as framboids vs. single crystals is controlled by the degree of supersaturation. Murowchick and Barnes (1987) demonstrated that degree of supersaturation controls pyrite morphology. Pyrite occurring as anhedral grains or angular particles is residual pyrite, remaining unoxidized in the tailings.

Calcite occurs as discrete particles exhibiting subrounded outlines, as rounded aggregates measuring 400 μm across, and as concentric shells. Calcite has porous-looking surfaces and commonly displays pitted and dissolved margins. Electron microprobe analysis indicates that calcite is relatively pure, with $MgCO_3$ and $FeCO_3$ contents less than 2 and 1 mol%, respectively. The occurrence of barite crystals as inclusions in calcite suggests that some calcite is a secondary mineral formed following barite precipitation. In addition, the occurrence of calcite in concentric shells similar to Fe-oxyhydroxide precipitates displaying colloidal textures suggests that some calcite in the tailings is secondary and formed within the tailings impoundment.

Another carbonate, calcian siderite occurs in the form of nodules measuring less than 10 μm across (Fig. 5b). Nodules occur as disseminations or clusters in cauliflower-like aggregates in Fe- and Fe-Si-oxyhydroxide precipitates (Fig. 5c). The Ca contents of calcian siderite appear to be variable from one nodule to another. Some calcian siderite nodules are zoned with higher Fe occurring in the center whereas others have calcite cores (Fig. 5d). Electron microprobe analysis indicates that calcian siderite contains up to 10 mol% $CaCO_3$ and 1 mol% $MnCO_3$. The texture of the calcian siderite points to a secondary origin. Minute particles of Fe-oxyhydroxide or Fe-oxide probably acted as the nucleation sites for the formation of the nodular siderite. Al et al. (2000) previously had reported secondary siderite coatings on ankerite grains in a tailings basin. The spatial distribution of secondary carbonates within the Lower Williams Lake tailings basin is shown on Figures 2, 3, and 6.

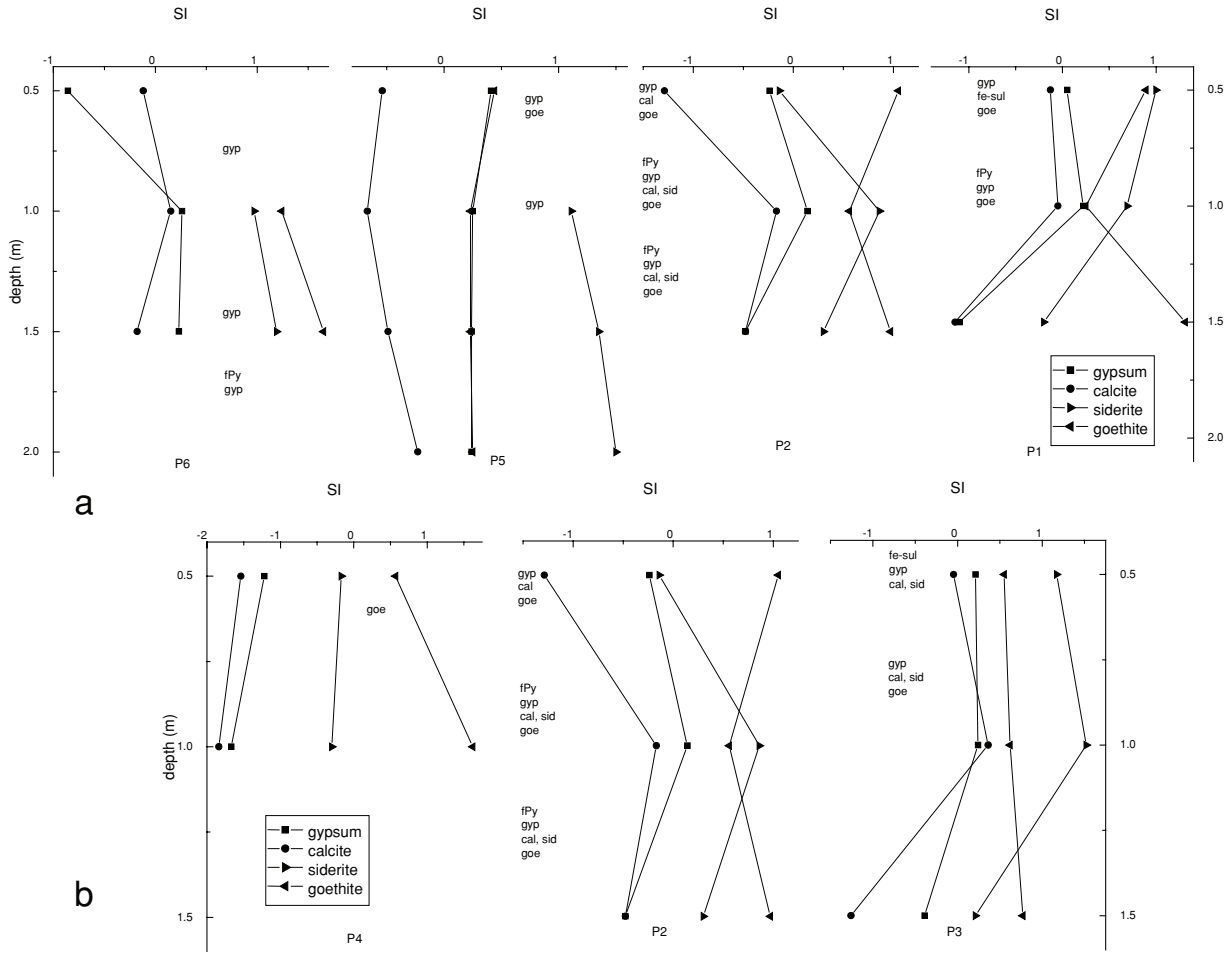

FIGURE 6. Variation of the saturation index (SI) with depth. SI values represent averages calculated from the measurements of November 18, 1996, June 4, 1997, June 27, 1997, and October 6, 1997. (**a**) Piezometers P1, P2, P5, and P6 along the W-E profile; (**b**) Piezometers P2, P3, and P4 along the N-S profile. Also shown are the relevant secondary minerals observed in cores (cal = calcite; fPy = framboidal pyrite; fe-sul = Fe sulfate; goe = goethite/Fe oxyhydroxide; gyp = gypsum; sid = calcian siderite).

Fe-oxyhydroxide and Fe-Si-oxyhydroxide occur as colloform-banded precipitates. The Fe-oxyhydroxides also occur as replacement products in cellular structures, probably representing pre-existing organic material (Fig. 4c), as irregularly shaped substances, and as matrix material to silicate mineral particles. Iron-oxyhydroxides were also observed as secondary oxidation layers on several pyrite grains in oxidized tailings close to the surface. Electron microprobe analyses of the Fe-oxyhydroxides indicate that Fe concentrations (as Fe_2O_3) are variable from 37 to 81 wt%. The Fe-oxyhydroxide grains at the lower end of this range contain up to 7% SiO_2, 2% Al_2O_3, 2% CaO, and 1% TiO_2. SiO_2 is present as chalcedony in banded textures and as a replacement product in cellular structures.

In addition to forming secondary product envelopes around pyrite particles, Fe-sulfate occurs as prismatic or fibrous crystals, and as a matrix to silicate minerals. Calcium sulfates are bassanite, gypsum, and anhydrite, which occur as small prismatic and fibrous crystals in minor to moderate concentrations. Gypsum and bassanite are secondary phases, probably formed within the tailings basin (Jambor 1994). Barite occurs as discrete particles and as inclusions in calcite and other secondary precipitates in the form of small, stubby to acicular prismatic crystals and as rosettes. Some composite particles contain up to 50% barite. Barite is a secondary phase and probably resulted from the $BaCl_2$ treatment of surface run-off to control Ra mobility into receiving streams.

Geochemistry

In general, groundwaters within the tailings contain high levels of potential total acidity, dissolved metals, sulfate, ammonia, chloride, and ^{226}Ra. Tailings at lower elevations and under permanent water cover contain higher levels of the contaminants. The pH of the groundwaters ranges from 5.8 to 11.3 and averages 6.7 (Table 1). The high pH values, in the 9.3–11.3 range, are observed at the P5 location at shallow depths, where unconsumed lime from previous sludge deposition or lime application is present. When these high values are excluded, the variation in pH is confined to 5.8–8.6, with an average value of 6.5. Dissolved sulfate, and total Fe and Ca concentrations are up to 2437, 503, and 950 mg/L, respectively.

TABLE 1. Saturation indices for sulfate, carbonate and Fe oxyhydroxide minerals in the groundwaters from the Lower Williams Lake tailings basin

Hole	depth (m)	date	*T*(°C)	pH	Eh (mV)	barite	gypsum	calcite	siderite	ferrihydrite	goethite
P1	0.5	Nov18,96	9.8	6.62	–48	–	0.04(0.05)	0.02(0.02)	1.46(1.33)	–2.10(4.25)	1.72(8.07)
P1	1.0	Nov18,96	10.4	6.77	–78	–	0.18	0.00	0.98	–2.57	1.27
P1	1.5	Nov18,96	15.1	6.53	62	–	–0.10	–0.66	0.02	–1.33	2.70
P1	0.5	Jun4,97	24.4	6.15	–63	0.58(0.63)	0.09(0.10)	–0.43(–0.43)	0.67(0.48)	–3.88(3.48)	0.49(7.85)
P1	1.0	Jun4,97	23.7	6.25	–125	0.27	0.21	–0.28	0.41	–4.98	–0.64
P1	1.5	Jun4,97	20.8	6.01	–25	0.24	–0.91	–1.27	–0.36	–4.34	–0.10
P1	1.0	Jun27,97	21.7	6.67	–128	0.43	0.24	0.04	0.76	–3.77	0.50
P1	1.5	Jun27,97	22.0	6.46	62	0.06	–0.39	–1.14	–0.01	–1.51	2.77
P1	0.5	Oct6,97	10.2	6.74	–111	0.52	0.01	0.01	0.88	–3.37	0.47
P1	1.0	Oct6,97	10.4	6.78	–143	0.52	0.26	0.03	0.60	–3.99	–0.15
P1	1.5	Oct6,97	10.8	6.29	–36	0.10	–1.98	–1.52	–0.46	–4.00	–0.14
P2	0.5	Nov18,96	14.1	6.38	–4	–	–0.12	–0.89	0.69	–2.01	1.98
P2	1.0	Nov18,96	15.4	6.67	–80	–	0.1(0.1)	0.02(0.02)	1.14(1.09)	–2.68(3.56)	1.35(7.6)
P2	1.5	Nov18,96	16.1	6.64	–49	–	–0.4	–0.26	0.5	–2.81	1.25
P2	0.5	Jun4,97	21.9	6.07	–55	0.74	–0.52	–1.39	–0.23	–4.29	–0.01
P2	1.0	Jun4,97	22.7	6.27	–125	0.34(0.2)	0.17(0.17)	–0.41(–0.41)	0.54(0.35)	–4.7(3.52)	–0.39(7.83)
P2	1.5	Jun4,97	25.8	6.18	–54	0.19	–0.49	–0.55	0.21	–4.16	0.25
P2	0.5	Oct6,97	10.8	5.96	83	1.65	–0.07	–1.6	–0.87	–2.67	1.19
P2	1.0	Oct6,97	7.7	6.7	–80	0.67	0.16	–0.17	0.82	–2.84	0.9
P2	1.5	Oct6,97	7.5	6.66	–76	0.55	–0.53	–0.69	0.03	–3.42	0.31
P2	1.0	Jun27,97	22.4	6.6	–141	0.48	0.11	–0.13	0.94	–3.92	0.38
P2	1.5	Jun27,97	22.8	6.52	–2	0.33	–0.49	–0.4	0.44	–2.27	2.05
P3	0.5	Nov18,96	16.6	6.73	–122	–	0.16(0.17)	0.25(0.24)	1.77(1.63)	–2.82(4.46)	1.27(8.54)
P3	1.0	Nov18,96	16.2	6.79	–128	–	0.22	0.56	1.84	–2.9	1.17
P3	1.5	Nov18,96	17.9	6.08	–34	–	–0.25	–1.12	0.27	–3.67	0.46
P3	0.5	Oct6,97	8.5	6.47	–103	0.41	0.27	–0.14	0.93	–3.71	0.06
P3	1.0	Oct6,97	10.4	6.5	–89	0.4	0.28	0.2	1.28	–3.37	0.48
P3	1.5	Oct6,97	8.5	6.4	–62	0.6	–0.44	–1.19	0.21	–3.44	0.33
P3	0.5	Jun4,97	26.3	6.2	–88	0.25	0.2	–0.26	0.81	–4.12	0.32
P3	1.0	Jun4,97	25.5	6.41	–105	–0.03	0.21	0.3	1.38	–3.73	0.68
P3	1.5	Jun4,97	26.6	5.8	–33	0.3	–0.44	–1.23	0.29	–3.62	0.83
P3	1.0	Jun27,97	22.1	6.58	–161	0.27	0.26	0.38	1.56	–4.13	0.16
P3	1.5	Jun27,97	22.7	5.9	41	0.44	–0.43	–1.48	0.08	–2.83	1.47
P4	0.5	Nov18,96	16.9	6.59	–82	–	–1.49(–1.48)	–1.32(–1.32)	0.36(0.29)	–3.14(3.27)	0.96(7.36)
P4	1.0	Nov18,96	18.1	6.68	–47	–	–0.81	–1.08	0.24	–2.39	1.75
P4	1.0	Oct6,97	9.8	6.72	–58	0.26	–1.76	–1.83	–0.21	–2.7	1.12
P4	0.5	Jun4,97	25.3	6.08	–39	0.42	–0.94	–1.76	–0.7	–4.22	0.18
P4	1.0	Jun4,97	22.8	6.13	–11	–0.21(–0.16)	–2.02(–2.03)	–2.21(–2.22)	–0.6(–0.64)	–3.56(2.13)	0.75(6.44)
P4	1.0	Jun27,97	22.9	6.27	87	–0.15	–2.07	–2.28	–0.62	–1.47	2.85
P5	0.5	Nov18,96	17.3	11.34	–91	–	0.51	2.04	–	–	–
P5	1.0	Nov18,96	18.7	6.48	–114	–	0.29	–0.46	1.13	–3.31	0.85
P5	1.5	Nov18,96	19.0	6.57	–139	–	0.22	–0.27	1.61	–3.24	0.93
P5	2.0	Nov18,96	19.0	6.56	–136	–	0.22	–0.19	1.65	–3.26	0.91
P5	0.5	Oct6,97	10.8	11.31	–230	0.68	0.41	0.21	–8.33	–0.95	2.91
P5	1.0	Oct6,97	10.2	6.63	–145	0.56	0.27	–0.52	1.24	–3.42	0.42
P5	1.5	Oct6,97	9.1	6.7	–153	0.66	0.28	–0.28	1.47	–3.35	0.44
P5	2.0	Oct6,97	9.6	6.77	–178	0.52(0.51)	0.26(0.28)	–0.05(–0.07)	1.59(1.34)	–3.65(4.88)	0.16(8.69)
P5	0.5	Jun4,97	29.5	6.1	10	0.45	0.31	–1.29	–1.32	–4.11	0.44
P5	1.0	Jun4,97	28.6	6.27	–135	0.3(0.24)	0.21(0.23)	–0.94(–0.96)	0.92(0.68)	–3.97(4.4)	0.55(8.92)
P5	1.5	Jun4,97	27.3	6.16	–152	0.27	0.2	–0.99	0.84	–4.63	–0.16
P5	2.0	Jun4,97	28.3	6.37	–171	0.15	0.22	–0.56	1.11	–4.42	0.08
P5	1.0	Jun27,97	23.4	6.22	–200	0.38	0.24	–0.77	1.14	–5.25	–0.91
P5	1.5	Jun27,97	23.4	6.46	–204	0.34	0.24	–0.42	1.47	–4.61	–0.28
P5	2.0	Jun27,97	23.2	6.52	–200	0.33	0.25	–0.12	1.63	–4.47	–0.15
P6	0.5	Oct6,97	12.8	8.63	–166	0.95	–1.1	0.66	–	–	–
P6	1.0	Oct6,97	13.8	7.27	–165	0.67	0.26	0.15	0.97	–2.74	1.24
P6	1.5	Oct6,97	13.0	7.55	–196	0.48(0.49)	0.25(0.25)	0.38(0.31)	1.71(1.48)	–1.95(5.01)	2(8.95)
P6	0.5	Jun4,97	28.3	6.82	–120	1.18	–0.62	–0.89	–	–	–
P6	1.5	Jun4,97	26.0	6.4	–76	0.94	0.21	–0.73	0.67	–3.13	1.29

Notes: Dashes = Corresponding chemical data not available. Numbers in parentheses are SI values where ferrous and ferric iron measurements are used in modeling. Eh values corrected to the standard hydrogen electrode potential.

Groundwaters from the deeper levels (e.g., 1.5 and 2 m) have lower sulfate concentrations in general. Groundwaters from the P4 location have the lowest Ca and SO_4 concentrations, whereas the P5 location has the highest.

Overall, saturation indices calculated for gypsum, calcite, siderite, and goethite are compatible with the secondary mineralogy of the tailings (Fig. 6). In addition, groundwaters in the tailings basin, including those of the sand unit underlying the basin, are saturated with respect to barite. This finding is in accordance with the common occurrence of barite in the tailings.

With a saturation index (SI) of approximately 0.25, most of the groundwaters are supersaturated with respect to gypsum (Table 1). Similarly, siderite saturation indices as high as 1.84 were calculated for some groundwaters. Based on error-propagation calculations, the effects of the analytical uncertainties on the SI values were found to be within ±0.02 for goethite, ±0.04 for gypsum, ±0.05 for barite, and ±0.20 for calcite and

siderite. As these values are much lower than the supersaturation levels, the uncertainties alone cannot account for the supersaturation. Another explanation could be the differences in the solubility-product values used in the calculations. For example, values for gypsum differ significantly in the MINTEQ and PHREEQ databases. The SI values for gypsum are reduced to near saturation levels when the solubility product in the PHREEQ database is used. Another cause could be the common-ion effect between gypsum, calcite, and barite on the one hand, and between siderite and goethite on the other.

The effect of Fe speciation based on Eh on siderite SI is small. When Fe^{2+} and Fe^{3+} concentrations are used in modeling, siderite SI is lowered by less than 0.2 (Table 1). Siderite supersaturation levels could also be due to the fact that siderite in the tailings is not pure but contains up to 20% Ca. Another factor could be the occurrence of calcian siderite in the form of fine-grained nodular or concretionary aggregates. Such forms of fresh precipitates are generally more soluble than the well-crystallized phases that are assumed by the geochemical modeling programs (Langmuir 1997).

In contrast to groundwater at the 0.5 and 1 m depths, groundwater at the 1.5 m depth at piezometer location P1 is undersaturated with respect to gypsum, calcite, and siderite (Fig. 6). At this depth, which is well below the interface between the tailings and the underlying sand and organics, saturation indices of both gypsum and calcite displayed a decrease with time (i.e., within ~11 month period). This effect could have arisen from dilution of downward-infiltrating sulfate and metal-rich tailings groundwater; dilution occurs because the regional groundwater flowing below the tailings and recharging the basin has an upward flow during the spring and fall recharge events. Whereas gypsum and goethite are present in the tailings at this site, secondary calcite and siderite were not observed.

Groundwaters at P2 are saturated with respect to gypsum at a depth of 1 m, but are undersaturated at 1.5 m and are nearly saturated at 0.5 m. Calcite is slightly below the saturation level. Both gypsum and calcite are present in the tailings at all depths, suggesting that these phases may dissolve with time.

In comparison to P2, groundwaters at P3 display slightly increased saturation levels for gypsum, calcite, and siderite at the 0.5 and 1 m depths. This could be a reflection of the localized northerly groundwater flow carrying dissolved constituents from the tailings at higher elevations to the nearby drainage ditch. Groundwater at the 1.5 m depth is undersaturated with respect to both gypsum and calcite. Goethite is saturated at all depths without any significant change in the saturation index with time.

Groundwaters, as sampled by P4 piezometers at 0.5 and 1 m depths during the spring and fall, are undersaturated with respect to gypsum and calcite. Tailings to the 0.5 m depth do not contain gypsum or calcite, in accord with the pore-water geochemistry. The water table rises to near the 0.5 m depth during wet periods and drops to near the 1 m depth during dry periods. Accordingly, gypsum or calcite, which may have been originally present in the tailings, probably dissolved and was removed. This may have a detrimental effect of enhanced ^{226}Ra mobility, which is controlled by the dissolved sulfate concentrations, hence through gypsum solubility.

Siderite supersaturation levels are characteristically the highest in the groundwaters at P5. Groundwater immediately below the sludge-tailings interface is undersaturated with respect to gypsum, whereas the deeper levels are saturated (Fig. 6). Mineralogy is in accord with the pore-water geochemistry in that the groundwaters of the tailings, but not those of the sludge, are saturated with respect to gypsum. Bottom water in the pond is saturated with respect to goethite and ferrihydrite but is undersaturated with respect to gypsum, calcite, and siderite.

Discussion

Formation of secondary minerals

Framboidal pyrite occurs in tailings mixed with the organic material sandwiched between the tailings on top and the organic-rich sand unit on the bottom, and toward the bottom of the main tailings (Fig. 2). The occurrence of framboidal pyrite in some of the Lower Williams Lake samples is unique in that it has been observed for the first time in samples taken from a tailings site having a well-established vegetation cover and a shallow water table.

Framboidal pyrite has been found to occur in modern sediments of anoxic basins and extreme saline environments, in continental margin and pelagic sediments, in sedimentary rocks, and in hydrothermal ores. Framboidal pyrite forms at a redox front from oxygen-bearing to hydrogen sulfide-bearing waters. Framboidal pyrite formation is a rapid process whereby single crystals of FeS form by direct precipitation from solution (Rickard 1974) and the reaction of FeS with aqueous H_2S produces framboidal pyrite (Rickard 1997; Rickard et al. 1997; Wilkin et al. 1996). According to Wilkin and Barnes (1997), framboidal pyrite forms as a result of initial nucleation and growth of an Fe monosulfide, reaction of the initial monosulfide to greigite (Fe_3S_4), aggregation of greigite microcrystals, and replacement of greigite by pyrite. The framboidal morphology is believed to result from the self-assembly of precursor greigite crystals due to their magnetic properties followed by replacement of progressively more S-rich phases: from disordered mackinawite to ordered mackinawite (Fe_9S_8) to greigite (Fe_3S_4) to pyrite (Wilkin et al. 1996), or from rapid nucleation in solutions that are supersaturated with respect to pyrite (Butler and Rickard 2000). If greigite is a precursor to the formation of pyrite, then the transformation occurred in neutral pH and slightly oxidizing conditions, because greigite has a narrow stability field in terms of Eh (above the H_2–H_2O line) and pH (5.9 to 7.4). Similarly, the formation of Fe monosulfides requires neutral and weakly alkaline conditions. According to Anderko and Shuler (1997), siderite may be a precursor for Fe sulfides, which require weakly alkaline conditions. The H_2S required in the formation of pyrite is produced as a result of bacterial sulfate reduction, which can be represented by the simple reaction:

$$2CH_2O + SO_4^{2-} \rightarrow 2HCO_3^- + H_2S \quad (1)$$

Interaction of H_2S with reactive detrital Fe minerals in reducing environments produces iron monosulfides; subsequently,

their reaction with elemental sulfur (Berner 1984; Berner 1970) or metastable S species such as polysulfides and thiosulfates (Wilkin and Barnes 1996; Wilkin and Barnes 1997; Langmuir 1997) forms pyrite.

The amount and reactivity of organic matter in the sediment place a major control on the rate of bacterial sulfate reduction in normal marine sediments (Berner 1984). The occurrence of cellular material in association with framboidal pyrite at the Lower Williams Lake site attests that organic matter was available and reducing conditions prevailed during the formation of secondary pyrite. Sulfate-reducing bacterial activity has been noted in anoxic zones of the Lower Williams Lake tailings and in tailings deposits elsewhere (Davé 1993; Fortin and Beveridge 1995; Gould et al. 1997). Sulfate reduction at the Lower Williams Lake was evidenced by the presence of a strong smell of H_2S gas during groundwater sampling. In contrast to marine sediments, sulfate is the principal species controlling pyrite formation in freshwater sediments because of the lower dissolved sulfate concentrations. In the Lower Williams Lake tailings basin, abundant sulfate is available as soluble gypsum and as the reaction products from pyrite oxidation. In addition to organic matter and sulfate, the amount and reactivity of detrital Fe minerals play an important role in the formation of pyrite. The Fe-oxyhydroxides, as highly reactive Fe minerals resulting from pyrite oxidation, provide an abundant supply of Fe in the Lower Williams Lake tailings.

An increased activity of Fe combined with an increase in CO_2 or HCO_3^-, resulting from the bacterial reduction of sulfate, may have promoted the precipitation of siderite. Calcite in the Lower Williams Lake tailings is relatively pure, containing less than 2 mol% $MgCO_3$ and 1 mol% $FeCO_3$. Secondary calcite occurring as a matrix to barite crystals contains 1 mol% $MgCO_3$ and 1 mol% $FeCO_3$. Siderite, on the other hand, contains up to approximately 10 mol% $CaCO_3$ and up to 5 mol% $MnCO_3$. Calcian siderite nodules are zoned, with higher Fe contents occurring in the center, which is similar to the zoning observed in siderite concretions in coal layers (Curtis et al. 1986). An exception to this is the occurrence of calcian siderite nodules with calcite cores observed in only one of the samples. This zoning probably reflects the changes in the composition of the groundwaters during the growth of the carbonate nodules. The Ca and Fe activities and precipitation of framboidal pyrite probably controlled the composition of the precipitating carbonate. Iron-poor carbonates would also precipitate from oxygenated waters because of the very low Fe_2O_3 solubility. Changes in the Ca and Fe concentrations in calcian siderite may have been due to the selective removal/depletion of one element over the other during the precipitation of carbonate and pyrite.

In the absence of sulfate reduction, the anaerobic sediment would support methanogenic microbial populations giving HCO_3^- and methane as principal products (Curtis et al. 1986) (reaction 2). As a result, alkalinity is increased and carbonate mineral precipitation is favored (reactions 3 and 4):

$$2CH_2O + H_2O \rightarrow HCO_3^- + CH_4 + H^+ \quad (2)$$

$$2Fe_2O_3 + CH_2O + 3H_2O \rightarrow HCO_3^- + 4Fe^{2+} + 7OH^- \quad (3)$$

$$Fe^{2+} + OH^- + HCO_3^- \rightarrow FeCO_3 + H_2O \quad (4)$$

Tailings groundwater within the basin is supersaturated with respect to siderite. This finding is similar to those of earlier geochemical studies at other tailings sites in the Elliot Lake area, where the tailings groundwater and groundwater in the neutral pH range were found to be supersaturated or near-saturated with respect to siderite (Morin et al. 1982; Dubrovsky et al. 1985). Morin and Cherry (1986) suspected the presence of calcite in an aquifer surrounding a tailings seepage and postulated the formation of siderite by calcite replacement to explain aqueous Fe losses in the aquifer. Blowes and Ptacek (1994) postulated that siderite saturation in the Elliot Lake tailings is caused by Fe^{2+} from sulfide oxidation and HCO_3^- released by the dissolution of calcite. However, the occurrence of secondary siderite was not confirmed by these researchers.

Overall decreases in the dissolved sulfate and Fe^{2+} concentrations with depth, and the saturation indices of siderite and calcite along P1, P2, P3, and P5, could be an indication of pyrite precipitation. In addition, groundwaters in the sand unit below the tailings as sampled by the piezometer nest at P1 display substantial decreases in sulfate concentration during the period from June to October. This depletion is independent of Ca; therefore, it cannot be attributed to dilution by groundwaters but perhaps to a mechanism that preferentially removes sulfate from the groundwater. It is conceivable that sulfate is removed by the action of sulfate-reducing bacteria that are most reactive during the summer months. Pyrite precipitation or reduction of sulfate in a groundwater saturated with respect to gypsum will cause gypsum to become undersaturated, and therefore, will promote gypsum dissolution. Calcite precipitation may accompany pyrite in such a case. Groundwaters at P5 display depletion of Ca with depth. The geochemical trends at the depth interval from 0.5 m to 1 m are suggestive of calcite precipitation. The trends are also suggestive of pyrite dissolution along the 1–1.5 m depth interval, and calcite dissolution and pyrite precipitation along the 1.5–2 m interval.

In summary, it is interpreted that sulfate originally produced from the oxidative dissolution of pyrite was reduced by bacteria in an organic-rich media and formed H_2S and HCO_3^-. The H_2S reacted with Fe oxyhydroxides to form framboidal pyrite through amorphous FeS and greigite. The bicarbonate generated during the bacterial reduction process reacted with Fe and/or Ca to form siderite and calcite.

Implications for reclamation

The occurrence of pyrite and carbonates as secondary minerals is significant as they are the first accounts of framboidal pyrite, siderite, and calcite formation in a tailings basin having a well-established vegetation cover and shallow water table. The presence of these secondary minerals suggests the establishment of favorable conditions within the saturated zone that are conducive to sulfate reduction and the precipitation of Fe sulfides. Organic carbon, sulfate-reducing bacteria, and the type of Fe-oxyhydroxide minerals are important factors in the formation of secondary pyrite and carbonate minerals. The site supports a well-established vegetation cover, and hence a con-

tinuous source of organic carbon is available through degradation of organic matter by both aerobic and anaerobic processes. Iron-oxyhydroxides are available through oxidation of original pyrite in the exposed tailings. The type of iron-oxyhydroxide is important for H_2S requirements in the reaction. Whereas low H_2S is adequate where amorphous ferrihydrite is the reactant, high H_2S concentrations will be needed for goethite as the principal reactant. Iron and bicarbonate concentrations, and Eh would limit the precipitation of carbonate.

The Lower Williams Lake tailings site is in its advanced stage of blending with the natural surroundings and is considered as a role model for environmental rehabilitation. The overall success of the basin is attributed to the covering of the tailings with a thick layer of glacial sand/gravel and till. This surface capping has helped in the establishment of a very successful vegetation cover, isolation of the deleterious effects of acid generating tailings to below the root zone and raising of the water table in the basin to above the tailings surface. The saturated conditions have created reducing conditions within the growth substrate, tailings and zones below, which in conjunction with the microbial degradation of the organic matter, both in the oxic and anoxic zones, are contributing to additional alkalinity in the tailings porewater and precipitation of secondary minerals that counter the previous oxidation history of the tailings. The tailings basin is a good candidate site where the evolution of environmental conditions can be studied. The existing conditions are desirable for the development of self-sustaining and ecologically blending habitats. Remediation and control actions may be designed to create similar conditions elsewhere to achieve environmentally acceptable tailings basins.

ACKNOWLEDGMENTS

The authors are grateful to Kevin Morin, Roger Smart, and Paul Weber for their diligent review and detailed comments on an earlier report on mineralogy. Valuable comments on the manuscript by John Dutrizac, John Jambor, and anonymous journal referees were greatly appreciated. Field and laboratory technical assistance were provided by Yvonne Boucher, Deborah Horne, Tjoe Lim, Mark Naklicki, Paul Carrière, Pierre Groulx, and the Analytical Services Group of CANMET. The financial support of Denison Mines Limited, Elliot Lake, Ontario, is acknowledged.

REFERENCES CITED

Al, T.A., Martin, C.J., and Blowes, D.W. (2000) Carbonate-mineral/water interactions in sulfide-rich mine tailings. Geochimica et Cosmochimica Acta, 64, 3933–3948.

Allison, J.D., Brown, D.S., and Novo-Gradac, K.J. (1991) MINTEQA2/PRODEFA2, a geochemical assessment model for environmental systems, Version 3.0 User's Manual. 106 p. EPA/600/3-91-021. U.S. EPA, Athens, Georgia.

Anderko, A. and Shuler, P.J. (1997) A computational approach to predicting the formation of iron sulfide species using stability diagrams. Computers and Geosciences, 23, 647–658.

Berner, R.A. (1984) Sedimentary pyrite formation: An update. Geochimica et Cosmochimica Acta, 48, 605–615.

———(1970) Sedimentary pyrite formation. American Journal of Science, 268, 1–23.

Blowes, D.W. and Ptacek, C.J. (1994) Acid-neutralization mechanisms in inactive mine tailings. In J.L. Jambor and D.W. Blowes, Eds., The Environmental Geochemistry of Sulfide Mine-Wastes, 438 p. Mineralogical Association of Canada, Ottawa, Ontario.

Butler, I.B. and Rickard, D. (2000) Framboidal pyrite formation via the oxidation of iron (II) monosulfide by hydrogen sulfide. Geochimica et Cosmochimica Acta, 64, 2665–2672.

Curtis, C.D., Coleman, M.L., and Love, L.G. (1986) Pore water evolution during sediment burial from isotopic and mineral chemistry of calcite, dolomite and siderite concretions. Geochimica et Cosmochimica Acta, 50, 2321–2334.

Davé, N.K. (1993) Panel Wetlands—A Case History of Partially Submerged Pyritic Uranium Tailings Underwater. Report prepared for Rio Algom Limited, Ontario Ministry of Northern Development and Mines (MNDM-MENDO) and the Mine Environmental Drainage (MEND) Program. Also Division Report, MSL 93-32 (CR).

Davé, N.K., Paktunc, A.D., and Nasserulla, S.M. (2000a). Geochemical evolution of Lower Williams Lake tailings basin, Elliot Lake, Ontario, Canada. In Proceedings of the Uranium 2000, International Symposium on the Process Metallurgy of Uranium, Saskatoon, Saskatchewan, Canada, September 9–15, 2000, p. 701–715. Canadian Institute of Mining, Metallurgy and Petroleum, Montreal, Canada.

———(2000b). Assessment of Physico-Chemical Stability of the Lower Williams Lake Tailings Basin, Denison Mines, Elliot Lake, Ontario. Division Report, MSL 2000-057 (CR).

Dubrovsky, N.M., Cherry, J.A., Reardon, E.J., and Vivyurka, A.J. (1985) Geochemical evolution of inactive pyritic tailings in the Elliot Lake uranium district. Canadian Geotechnical Journal, 22, 110–128.

Fortin, D. and Beveridge, T.J. (1995) Presence of sulfate-reducing bacteria in two sulfidic mine tailings and their potential role in the formation of diagenetic iron sulfide minerals. In L. Lortie, W.D. Gould, and S. Rajan, Eds., Biotechnology and the Mining Environment. Proceedings of the Eleventh Annual General Meeting of BIOMINET, CANMET-Natural Resources Canada, 87–101.

Gould, W.D., Francis, M., Blowes, D.W., and Krouse, H.R. (1997) Biomineralization: Microbiological formation of sulfide minerals. In J.M. McIntosh and L.A. Groat, Eds., Biological–Mineralogical Interactions, 25, p. 169–186. Mineralogical Association of Canada, Ottawa, Ontario.

Jambor, J. (1994) Mineralogy of sulfide-rich tailings and their oxidation products. In J.L. Jambor and D.W. Blowes, Eds., The Environmental Geochemistry of Sulfide Mine-Wastes, Chapter 3, p. 59–122. Short Course Handbook, Ottawa, Ontario.

Langmuir, D. (1997) Aqueous Environmental Geochemistry, 600 p. Prentice Hall, New Jersey.

Morin, K.A. and Cherry, J.A. (1986) Trace amounts of siderite near a uranium-tailings impoundment, Elliot Lake, Ontario, Canada, and its implication in controlling contaminant migration in a sand aquifer. Chemical Geology, 56, 117–134.

Morin, K.A., Cherry, J.A., Lim, T.P., and Vivyurka, A.J. (1982) Contaminant migration in a sand aquifer near an inactive tailings impoundment, Elliot Lake, Ontario. Canadian Geotechnical Journal, 19, 49–62.

Murowchick, J.B. and Barnes, H.L. (1987) Effects of temperature and degree of supersaturation on pyrite morphology. American Mineralogist, 72, 1241–1250.

Paktunc, A.D. and Davé, N.K. (1999) Mineralogical characterization of pyritic uranium tailings from the Lower Williams Lake tailings basin, Denison Mines, Elliot Lake, Ontario. CANMET, Mining and Mineral Sciences Laboratories report MMSL 99-054(CR).

Parkhurst, D.L. (1995) PHREEQC—A computer program for speciation, reaction-path, advective-transport, and inverse geochemical calculations. U.S. Geological Survey Water Resources Inventory, 95–4227.

Rickard, D. (1974) Kinetics and mechanism of the sulfidation of goethite. American Journal of Science 274, 941–952.

———(1997) Kinetics of pyrite formation by the H_2S oxidation of iron (II) monosulfide in aqueous solutions between 25 and 125 °C: The rate equation. Geochimica et Cosmochimica Acta, 61, 115–134.

Rickard, D. and Luther, G.W. III (1997) Kinetics of pyrite formation by the H_2S oxidation of iron (II) monosulfide in aqueous solutions between 25 and 125 °C: The mechanism. Geochimica et Cosmochimica Acta, 61, 135–147.

Wilkin, R.T. and Barnes, H.L. (1996) Pyrite formation by reactions of iron monosulphides with dissolved inorganic and organic sulphur species. Geochimica et Cosmochimica Acta, 60, 4167–4179.

———(1997) Formation of framboidal pyrite. Geochimica et Cosmochimica Acta, 61, 323–339.

Wilkin, R.T., Barnes, H.L., and Brantley, S.L. (1996) The size distribution of framboidal pyrite in modern sediments: An indicator of redox conditions. Geochimica et Cosmochimica Acta, 60, 3897–3912.

MANUSCRIPT RECEIVED JULY 31, 2001
MANUSCRIPT ACCEPTED JANUARY 17, 2002
MANUSCRIPT HANDLED BY GERALD GIESTER